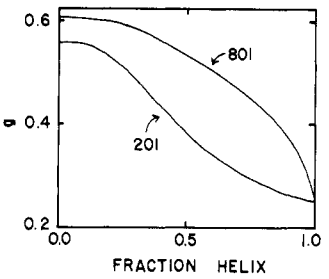

Figure 5. Comparison of the relationship between g and helical content when $\sigma = 0.00068$ and n_p is 201 or 801. The cross-link occurs between the central amino acid residues in two identical polypeptide chains.

The relationship between g and helical content for $n_p = 201$ and 801 is compared in Figure 5. If any disorder is present, g for $n_p = 801$ will exceed g for $n_p = 201$. The contrast is particularly striking when helical contents exceed 0.20. These effects have their origin in the increasing sensitivity of the unperturbed dimensions of predominately helical molecules to residual disorder as n_p increases and the fact that an n_p of 201 is insufficient to produce the asymptotic g for completely disordered molecules. In general, the true g and f_1 for partially helical polypeptides will lie between the limits defined by random-flight statistics and rigid rod behavior.

Implications for Cross-Linked Proteins. Proteins will differ from the homopolypeptides considered here in that 20 amino acid residues with different σ and s will be present. Homopolypeptides always have their highest helix-forming tendency in the middle of the polypeptide chain, while the chain ends tend to be disordered. In contrast, the amino acid sequence of a protein may yield maximal helix-forming tendencies at locations remote from the middle of a polypeptide chain. Those proteins which contain propyl residues will possess sites at which propagation of an α helix is extremely difficult, a feature not found in poly(hydroxybutyl-L-glutamine). Consequently the results presented here will not be expected to apply to any particular partially helical, cross-linked protein. The important conclusion to be drawn is that there is little reason to anticipate that random-flight statistics will be applicable to the estimation of the effect of cross-linking on the unperturbed dimensions of partially helical proteins. This problem must be approached using rotational isomeric state theory.

Acknowledgment. Supported in part by National Science Foundation Grants DMB-73-07655 A02 and PCM76-23235 and by a fellowship from the John Simon Guggenheim Memorial Foundation. This work was conducted while on sabbatical leave at the Department of Chemistry, Stanford University. The author wishes to thank Dr. Flory for his hospitality during this period.

References and Notes

(1) M. O. Dayhoff, Ed., "Atlas of Protein Sequence and Structure", Vol. 5, The National Biomedical Research Foundation, Silver Spring, Md., 1972.
(2) R. Chalkley and C. Hunter, *Proc. Natl. Acad. Sci. U.S.A.*, **72**, 1304 (1975).
(3) J. O. Thomas and R. D. Kornberg, *Proc. Natl. Acad. Sci. U.S.A.*, **72**, 2626 (1975).
(4) H. G. Martinson, M. D. Shetlar, and B. J. McCarthy, *Biochemistry*, **15**, 2002 (1976).
(5) H. G. Martinson and B. J. McCarthy, *Biochemistry*, **15**, 4126 (1976).
(6) R. Osterberg, B. Sjoberg, A. Liljas, and I. Petterson, *FEBS Lett.*, **66**, 48 (1976).
(7) T. H. Ji and I. Ji, *J. Mol. Biol.*, **86**, 129 (1974).
(8) C. Tanford, *Adv. Protein Chem.*, **23**, 121 (1968).
(9) W. L. Mattice, J. M. Riser, and D. S. Clark, *Biochemistry*, **15**, 4264 (1976).
(10) B. H. Zimm and W. H. Stockmayer, *J. Chem. Phys.*, **17**, 1301 (1949).
(11) W. L. Mattice, *Macromolecules*, **10**, 511 (1977).
(12) W. L. Mattice and D. K. Carpenter, *Macromolecules*, **9**, 53 (1976).
(13) W. L. Mattice, *Macromolecules*, **10**, 516 (1977).
(14) B. H. Zimm and J. K. Bragg, *J. Chem. Phys.*, **31**, 526 (1959).
(15) P. H. von Dreele, N. Lotan, V. S. Ananthanarayanan, R. H. Andreatta, D. Poland, and H. A. Scheraga, *Macromolecules*, **4**, 408 (1971).
(16) W. L. Mattice, *Macromolecules*, **8**, 644 (1975).
(17) W. L. Mattice, *Macromolecules*, **9**, 48 (1976).
(18) D. A. Brant, W. G. Miller, and P. J. Flory, *J. Mol. Biol.*, **23**, 47 (1967).
(19) G. N. Ramachandran and V. Sasisekharan, *Adv. Protein Chem.*, **23**, 284 (1968).
(20) P. J. Flory, *Macromolecules*, **7**, 381 (1974).
(21) D. A. Brant and P. J. Flory, *J. Am. Chem. Soc.*, **87**, 663 (1965).
(22) W. G. Miller and P. J. Flory, *J. Mol. Biol.*, **15**, 298 (1966).

Conformation of Hydrocarbon Chains Attached to a Planar Chromophore. A Monte-Carlo Study

Douglas S. Saunders[12] and Mitchell A. Winnik*

Lash Miller Laboratories and Departments of Chemistry, Erindale College and University of Toronto, Toronto, Ontario, Canada M5S 1A1. *Received June 23, 1977*

ABSTRACT: A diamond-lattice model and Monte-Carlo methods are used to simulate the conformational properties of hydrocarbon chains up to 30 carbons in length attached via an ester group to an aromatic chromophore. The chromophore was modeled in the lattice by specifying as occupied those lattice sites which best specify its geometry. Chains attached to the chromophore were examined for the case of second neighbor exclusion and with appropriate Boltzmann factors to simulate temperature effects on chain properties. Various properties of the chains were examined, including first, second, and fourth moments of the end-to-end vector **r**, and its projections onto the principal axes of a Cartesian coordinate system centered at C(1) of the chain. Values of the distribution of the end-to-end vector are reported for 10-, 20-, and 30-carbon chains as the projections of **r** onto the principal axes. Where comparison is possible with similar calculations on unsubstituted polymethylene chains, the effect of the chromophore on these properties of the chains is seen to be small.

When a hydrocarbon chain is attached to a bulky substituent, its conformational properties are affected. The steric effect of the substituent excludes a certain volume of space, and this in turn should perturb various conformational properties of the chains. The effect of the substituent on chain properties might vary with chain length, with temperature, with the shape of the substituent, and with the interaction potential between the substituent and the chain.

0024-9297/78/2211-0018$01.00/0

Conformational calculations based upon fairly simple models can be very useful for gaining insights into properties of chain molecules which cannot be obtained experimentally. The key to many conformationally dependent properties of polymers is the distribution function for the end-to-end vector,[1] **r**. For long polymers in theta solvents, the distribution function is Gaussian in form. For short chains, the distribution of **r** is no longer Gaussian.[2] It may not be spherically or cylindrically symmetric about the axes of some internal Cartesian coordinate system. The situation is rather complex, and the complications become more pronounced with the presence of the terminal substituent.

The conformational properties of chains attached to large substituents are important in two respects. First, the steric effect of a substituent is a form of excluded volume. Exploring its influence on the properties of chains attached to it is a way of assessing which aspects of the conformation of short chains are sensitive to excluded volume. Second, a number of experiments have been published recently which involve molecules containing both a hydrocarbon chain and terminal chromophoric substituents.[3] Models which can accommodate one or two large chromophores attached to the ends of flexible chains are necessary to simulate those experimental phenomena.

As a first step toward understanding the effects of substituents on the conformational properties of short chains attached to bulky substituents, we examine aspects of the conformation of the hydrocarbon chains in the molecule **1**. Cyclization in **1** has been considered separately.[4] In this paper

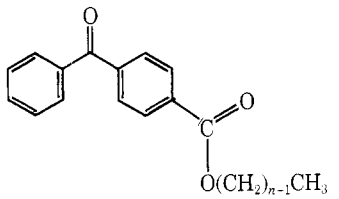

1

we examine moments of the end-to-end vector as a function of temperature for chain lengths up to 30 carbons in length and their distribution functions. In addition we describe the effect of the chromophore on the fraction of trans bonds in the chain.

Methodology

When one wishes to simulate experimental phenomena associated with molecule **1**, both syn and anti rotamers of the ester group need to be considered. The conformational properties of chains attached to each would then be averaged. In this work, where we are concerned with the conformational properties of a chain attached to a substituent, we need to consider only one rotamer. We have arbitrarily chosen to examine the anti form of the ester. Examining the syn form is in principle akin to studying a different substituent at the chain terminus and is beyond the scope of the present work.

The model involves random walks on a diamond lattice with second neighbor exclusions. The terminal substituent is modeled in the lattice by designating as occupied those lattice sites which best simulate its shape. The structural parameters of the chain are introduced in a semiempirical manner. These are described in the following paper.[4,5]

Random samples of molecular configurations were generated stepwise from C_1 until either the chain was trapped or until it reached 30 carbons. The sampling technique of Rosenbluth and Rosenbluth[6a] was employed. In this approach, each step in a growing walk is assigned a step weight w_j equal to the reciprocal of the probability of taking that step. The counting weight of the l'th chain of length n, $W_l^{(n)}$, is the

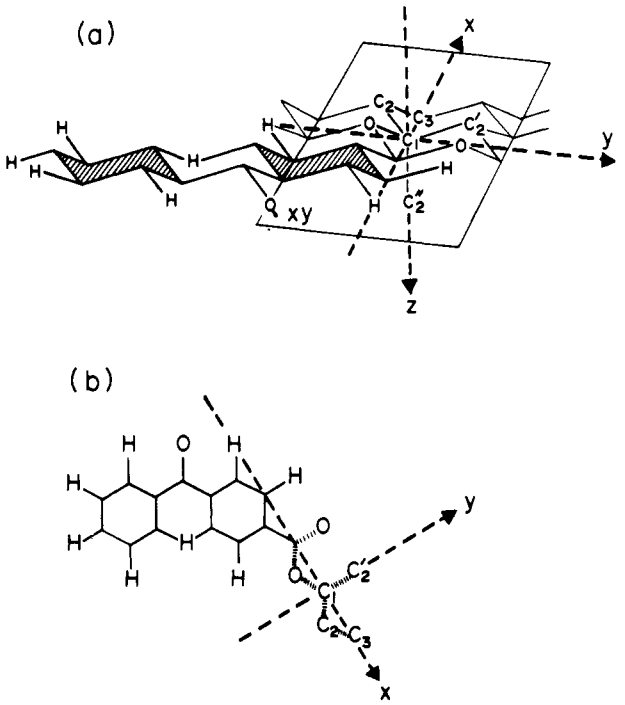

Figure 1. Diamond-lattice model of benzophenone-4-$(CH_2)_{n-1}CH_3$ showing the coordinate system used in the calculation of first moments of the projections of the end-to-end vector and their distribution functions. The coordinate axes are shown as heavy dashed lines. The chromophore lies in the x,y plane. The anti configuration of the ester group is shown. In (a) the simulated aromatic rings are shaded. Portions of the diamond lattice are drawn, and the x,y plane is indicated. Also shown are the three possible loci for C_2. In (b) the projection of the chromophore onto the x,y plane is depicted. The bonds O||||C imply that the ester and chain atoms not on the x axis lie below the plane in the $-z$ direction.

product of the step weights over the $(n-1)$ bonds times the Boltzmann factor associated with the conformational energy E_j of that step.

$$W_l^{(n)} = \prod_{j=1}^{n-1} W_{l,j} \exp(-E_j/kT) \tag{1}$$

Properties of the chains were calculated from eq 2 where the estimated mean of a property ν, $\langle\hat{\nu}\rangle$, is obtained from a sample of N chains, and $\nu_l^{(n)}$ is the value of the property for the l'th chain of length n in the sample. The estimated partition function $\langle\hat{Z}^{(n)}\rangle$ for chains of length n is given by eq 3.

$$\langle\hat{\nu}^{(n)}\rangle = \sum_{l=1}^{N} \nu_l^{(n)} W_l^{(n)} \Big/ \sum_{l=1}^{N} W_l^{(n)} \tag{2}$$

$$\langle\hat{Z}^{(n)}\rangle = \frac{1}{N} \sum_{l=1}^{N} W_l^{(n)} \tag{3}$$

A sample of 180 000 chains was generated. Chains were grown with the constraint that $E_t = E_g$. Properties of chains at real temperatures were obtained by reweighting the data according to eq 1 and 2. To calculate the variance of estimates of chain properties, the sample was divided into eight groups of 22 500 chains. These were analyzed by the procedure proposed by McCrackin.[6b]

Results and Discussion

The Coordinate System. Traditionally, various vectorial properties of unsubstituted polymers are examined within the context of a Cartesian coordinate system which takes the first bond along the x axis and the second bond in the x,y plane.[1] The presence of a terminal substituent destroys the simplicity of this frame of reference. One needs a coordinate system

Table I
Averaged *x*, *y*, and *z* Coordinates of the End-to-End Vector[a]

Chain length	$E_t = E_g$			140 °C			25 °C		
	$\langle r_x \rangle$	$\langle r_y \rangle$	$\langle r_z \rangle$	$\langle r_x \rangle$	$\langle r_y \rangle$	$\langle r_z \rangle$	$\langle r_x \rangle$	$\langle r_y \rangle$	$\langle r_z \rangle$
2	0.42	0.24	−0.17	0.60	0.03	−0.02	0.68	−0.05	0.04
3	0.78	0.09	−0.26	1.20	0.05	−0.15	1.35	0.04	−0.12
4	1.03	0.09	−0.20	1.56	0.07	−0.16	1.78	0.04	−0.12
5	1.35	0.12	−0.35	1.98	0.08	−0.22	2.26	0.07	−0.17
6	1.59	0.12	−0.34	2.30	0.12	−0.25	2.63	0.11	−0.21
7	1.81	0.21	−0.39	2.60	0.17	−0.28	2.98	0.16	−0.24
8	1.96	0.22	−0.41	2.83	0.20	−0.31	3.25	0.19	−0.27
9	2.11	0.25	−0.44	3.02	0.25	−0.33	3.47	0.25	−0.29
10	2.24	0.27	−0.45	3.20	0.28	−0.34	3.68	0.28	−0.30
11	2.38	0.30	−0.47	3.37	0.31	−0.33	3.88	0.31	−0.26
12	2.48	0.33	−0.48	3.50	0.34	−0.33	4.04	0.35	−0.27
13	2.60	0.36	−0.50	3.67	0.36	−0.35	4.24	0.37	−0.28
14	2.68	0.38	−0.50	3.77	0.38	−0.33	4.38	0.38	−0.26
15	2.77	0.41	−0.51	3.90	0.40	−0.36	4.56	0.40	−0.31
16	2.84	0.43	−0.52	4.01	0.42	−0.38	4.67	0.43	−0.33
17	2.91	0.45	−0.53	4.08	0.41	−0.42	4.74	0.39	−0.43
18	2.97	0.46	−0.53	4.19	0.39	−0.42	4.91	0.34	−0.42
19	3.03	0.48	−0.54	4.25	0.45	−0.41	4.96	0.43	−0.37
20	3.07	0.50	−0.54	4.32	0.46	−0.45	5.06	0.42	−0.46
21	3.12	0.52	−0.55	4.37	0.52	−0.49	5.12	0.51	−0.54
22	3.16	0.54	−0.55	4.41	0.53	−0.50	5.16	0.44	−0.59
23	3.21	0.56	−0.55	4.44	0.52	−0.50	5.24	0.47	−0.60
24	3.23	0.58	−0.55	4.32	0.58	−0.43	5.07	0.40	−0.41
25	3.26	0.60	−0.55	4.32	0.58	−0.40	4.81	0.50	−0.34
26	3.28	0.63	−0.56	4.28	0.67	−0.48	4.74	0.69	−0.58
27	3.31	0.64	−0.56	4.29	0.58	−0.52	4.79	0.44	−0.61
28	3.34	0.64	−0.56	4.40	0.54	−0.50	5.11	0.33	−0.61
29	3.36	0.66	−0.56	4.32	0.57	−0.51	4.81	0.29	−0.67
30	3.38	0.67	−0.56	4.24	0.60	−0.46	4.56	0.36	−0.57

[a] Estimated standard deviations are 1 to 3% for $E_t = E_g$; for 140 °C, $\sigma(r_x)$ is 3 to 5%, $\sigma(r_y)$ and $\sigma(r_z)$ are 15 to 30% of the estimated value; for 25 °C, $\sigma(r_x)$ is 3 to 8%, $\sigma(r_y)$ and $\sigma(r_z)$ are 15 to 20% for $n \leq 18$, about 50% for $20 \leq n \leq 26$, and nearly 100% for $n = 30$.

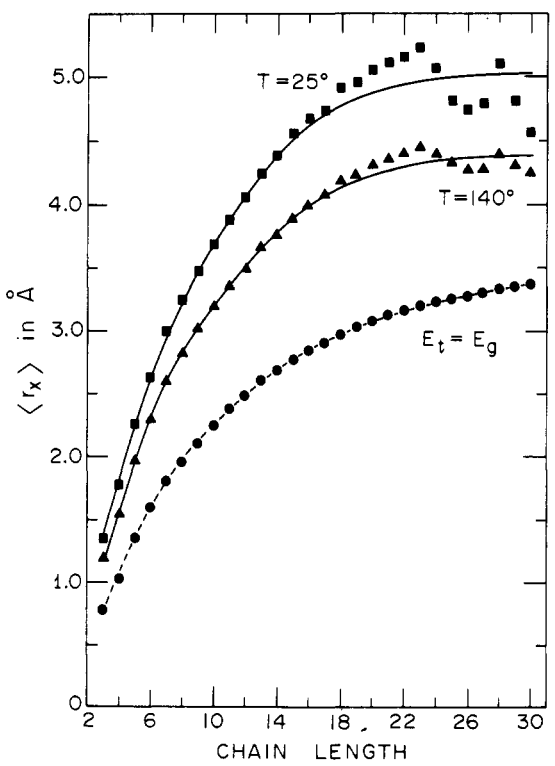

Figure 2. The estimated average projection of the end-to-end vector onto the x axis, $\langle \mathbf{r}_x \rangle$, as a function of chain length and temperature. For the lowermost line $E_t = E_g$. For the upper lines $E_g = E_t + 500$ cal/mol at 140 and 25 °C, respectively.

which simplifies as much as possible the interpretation of chain properties which may result from interaction between the substituent and the chain.

We have chosen the plane of the chromophore as the x,y plane in a Cartesian coordinate system which has the x axis chosen to pass through the carbonyl carbon of the ester and C_1 of the polymethylene chain. This axis contains alternate atoms of the all-trans chain which is also trans about the C–O bond. C_1 is chosen as the origin. The positive x, y, and z directions are as indicated in Figure 1.

From C_1 there are three possible loci for the second carbon in the chain. The bond to C_2 lies at an angle of 35.25° to the x axis, that to C_2' lies in the y,z plane, and that to C_2'' lies along the $+z$ axis. Thus the y,z plane bisects the $\angle OC_1C_2$ angle, and within the x,y plane, the substituent lies in the $(-x, -y)$ quadrant.

The First Moment. The projection of the end-to-end vector **r** onto the first bond in a polymer chain is known as the persistence vector.[1,2b] The magnitude of the persistence vector **a** as a function of chain length is usually interpreted as one description of the extent to which bonds in the chain are correlated with the direction of the first bond vector in the chain.

Because of the presence of the substituent, there are three different positions for the bond vector that joins C_2 to the origin. A true persistence vector cannot be defined for this coordinate system. Consequently we report simply the first moments of **r**, the averaged projections of the end-to-end vector $\langle \mathbf{r}_x \rangle$, $\langle \mathbf{r}_y \rangle$, $\langle \mathbf{r}_z \rangle$ on each of the axes of our coordinate system.

Values of $\langle \mathbf{r}_x \rangle$, $\langle \mathbf{r}_y \rangle$, and $\langle \mathbf{r}_z \rangle$ for chain lengths up to 30 carbons are collected in Table I for three temperatures: $\infty(E_t$

Table II
Values of $\langle r^2 \rangle$, $\langle r_i^2 \rangle$, and $\langle r_i^4 \rangle$ for $E_t = E_g$

Chain length	$\langle r^2 \rangle$, Å^2	$\langle r_i^2 \rangle$, Å^2			$\langle r_i^4 \rangle$, Å^4		
	$\langle r^2 \rangle^a$	$\langle r_x^2 \rangle^b$	$\langle r_y^2 \rangle$	$\langle r_z^2 \rangle$	$\langle r_x^4 \rangle^c$	$\langle r_y^4 \rangle$	$\langle r_z^4 \rangle$
2	2.37	0.53	0.88	0.97	0.83	1.57	1.93
3	6.32	1.77	1.91	2.64	6.52	6.83	11.13
4	10.89	3.09	3.51	4.30	20.48	23.70	35.05
5	18.25	5.28	5.88	7.09	57.85	65.45	90.40
6	26.37	7.76	8.56	10.05	122.05	138.12	182.24
7	35.54	10.57	11.53	13.44	226.96	253.75	325.60
8	45.46	13.68	14.85	16.93	376.21	421.92	523.46
9	56.01	16.98	18.30	20.73	581.66	645.56	789.72
10	67.18	20.52	22.07	24.59	852.20	941.99	1123.7
11	79.02	24.21	25.98	28.83	1194.0	1315.8	1554.6
12	91.12	28.06	30.40	33.02	1614.1	1773.0	2064.4
13	103.8	32.11	34.19	37.54	2127.5	2321.7	2687.5
14	116.7	36.12	38.57	41.97	2712.9	2975.1	3387.4
15	129.9	40.42	42.94	46.57	3416.4	3718.6	4208.4
16	143.4	44.74	47.37	51.26	4216.9	4568.6	5152.4
17	157.2	49.18	52.01	56.04	5119.0	5547.9	6206.6
18	171.2	53.67	56.70	60.83	6142.9	6653.4	7379.7
19	185.6	58.37	61.43	65.78	7308.9	7879.8	8707.5
20	199.7	62.93	66.14	70.65	8560.8	9179.2	10117.0
21	214.3	67.70	70.95	75.66	9961.1	10646.0	11696.0
22	229.0	72.48	75.85	80.64	11496.0	12256.0	13378.0
23	244.1	77.42	80.91	85.75	13187.0	14039.0	15229.0
24	259.0	82.15	85.99	90.84	14923.0	15959.0	17238.0
25	274.4	87.27	91.07	96.05	16877.0	18018.0	19412.0
26	289.4	92.23	96.03	101.17	18953.0	20183.0	21669.0
27	304.7	97.35	101.0	106.3	21187.0	22535.0	24091.0
28	320.6	102.5	106.6	111.5	23618.0	25029.0	26628.0
29	336.5	107.8	111.8	116.9	26249.0	27654.0	29450.0
30	352.2	113.0	117.0	122.2	28962.0	30441.0	32366.0

[a] $\langle r^2 \rangle = \langle r_x^2 \rangle + \langle r_y^2 \rangle + \langle r_z^2 \rangle$. [b] $\langle r_x^2 \rangle$ is the second moment of the x coordinate of the end-to-end vector **r**. [c] $\langle r_x^4 \rangle$ is the fourth moment of the x coordinate of the end-to-end vector **r**. Estimated standard deviations are 1 to 3% of the values shown.

Table III
Values of $\langle r^2 \rangle$, $\langle r_i^2 \rangle$, and $\langle r_i^4 \rangle$ at 25 °C

Chain length	$\langle r^2 \rangle$, Å^2	$\langle r_i^2 \rangle$, Å^2			$\langle r_i^4 \rangle$, Å^4		
	$\langle r^2 \rangle^a$	$\langle r_x^2 \rangle^b$	$\langle r_y^2 \rangle$	$\langle r_z^2 \rangle$	$\langle r_x^4 \rangle^c$	$\langle r_y^4 \rangle$	$\langle r_z^4 \rangle$
2	2.37	0.85	0.77	0.75	1.34	1.17	1.36
3	6.32	2.84	1.65	1.83	13.61	6.50	7.79
4	12.36	5.14	3.35	3.65	48.55	25.95	31.87
5	20.34	8.56	5.67	6.11	130.33	70.05	82.33
6	29.73	12.20	8.45	9.08	268.26	153.57	181.23
7	40.67	16.45	11.69	12.53	494.06	289.16	332.56
8	52.56	20.78	15.36	16.42	800.15	495.00	571.45
9	65.18	25.24	19.31	20.64	1193.2	770.76	885.54
10	78.63	29.90	23.58	25.14	1700.8	1144.4	1308.4
11	93.18	35.08	28.16	29.94	2390.6	1630.2	1847.7
12	107.8	40.11	32.80	34.85	3161.8	2212.0	2513.4
13	123.5	45.87	37.56	40.05	4199.5	2919.9	3325.7
14	138.8	51.25	42.57	44.99	5304.6	3765.1	4191.3
15	155.8	57.60	47.37	50.82	6756.6	4664.5	5347.1
16	172.5	62.89	53.02	56.59	8132.3	5871.1	6649.2
17	188.6	68.22	58.04	62.35	9748.3	7083.0	8028.3
18	206.1	75.59	63.04	67.48	12295.0	8536.8	9497.2
19	223.6	81.41	68.71	73.52	14198.0	10083.0	11343.0
20	240.6	87.50	74.27	78.81	16274.0	11699.0	13009.0
21	257.0	93.12	79.52	84.37	18506.0	13619.0	14936.0
22	274.7	99.36	86.31	89.04	21234.0	16300.0	16625.0
23	294.0	106.9	90.78	96.37	24903.0	18187.0	10230.0
24	313.1	111.6	98.12	103.4	27470.0	21519.0	22521.0
25	329.2	115.9	103.9	109.4	30311.0	24010.0	25641.0
26	344.8	119.5	109.8	115.5	32929.0	27078.0	28907.0
27	363.6	126.5	115.8	121.3	37836.0	29927.0	31712.0
28	388.5	139.8	123.8	125.0	47296.0	34156.0	33436.0
29	402.6	141.2	128.3	133.1	48150.0	36734.0	38103.0
30	412.6	142.1	132.4	138.1	49650.0	40004.0	42223.0

[a] $\langle r^2 \rangle = \langle r_x^2 \rangle + \langle r_y^2 \rangle + \langle r_z^2 \rangle$. [b] $\langle r_x^2 \rangle$ is the second moment of the x coordinate of the end-to-end vector **r**. [c] $\langle r_x^4 \rangle$ is the fourth moment of the x coordinate of the end-to-end vector **r**. Estimated standard deviations are 5 to 10% of the values shown.

$= E_g$), 140 °C, and 25 °C. The value of $\langle \mathbf{r}_x \rangle$ is large: more that two bonds for a 30-carbon chain when $E_g = E_t$, and more than three bonds at 25 °C. Values of $\langle \mathbf{r}_y \rangle$ are much smaller; the persistence in the y direction is less than half a bond length for 30-carbon chains and even less for shorter chains. Values of $\langle \mathbf{r}_z \rangle$ are also small and negative. As the temperature is lowered, the magnitude of $\langle \mathbf{r}_x \rangle$ increases markedly while that of $\langle \mathbf{r}_y \rangle$ decreases. The temperature and chain length dependence of $\langle \mathbf{r}_x \rangle$ are plotted in Figure 2.

One interesting feature of Figure 2 is that when $E_t = E_g$, $\langle \mathbf{r}_x \rangle$ has not levelled off even for 30-carbon chains. This implies that the direction of the 29'th bond in the chain is still sensitive to the orientation of the chromophore and of the first bonds in the chain. This result is similar to that of Yoon and Flory,[2b] who found for unsubstituted polymethylene chains (using a different model and another coordinate system) that $\mathbf{a}_x$ and $\mathbf{a}_y$ increased only slightly above 25-carbon chains. Because of the three directions possible for the bond between C(1) and C(2), the magnitude of the first moment we calculate for substituted chains is *smaller* than the corresponding persistence vector for polymethylene chains of the same length calculated by Yoon and Flory. The magnitude of $\langle \mathbf{r}_x \rangle$ increases with a decrease in temperature as trans conformations of the chain become increasingly favored. Scatter in the data for chains longer than 20 carbons makes it impossible to comment on the effect of temperature on the tendency of $\langle \mathbf{r}_x \rangle$ to level off for long chains.

The most interesting feature of the data is the large difference in the $\langle \mathbf{r}_x \rangle$ and $\langle \mathbf{r}_y \rangle$ values. These suggest that the end-to-end vector is much more sensitive to stereochemical features adjacent to the origin (the ester group) than to the orientation of the chromophore several bonds removed.

The Second and Fourth Moments of r. The second moment of the end-to-end vector $\langle r^2 \rangle$ can be considered in terms of its components $\langle r_x^2 \rangle$, $\langle r_y^2 \rangle$, and $\langle r_z^2 \rangle$. The extent to which these components are equal in magnitude gives some indication of how symmetrically $\mathbf{r}$ is disposed about the origin. A similar qualitative picture comes out of a comparison of $\langle r_x^4 \rangle$, $\langle r_y^4 \rangle$, and $\langle r_z^4 \rangle$ with more extended chains counting more heavily in the averages. These values are presented in Table II for $E_t = E_g$ and in Table III for 25 °C. For chains under 10 carbons, when $E_t = E_g$, $\langle r_z^2 \rangle$ is significantly larger than $\langle r_y^2 \rangle$, which in turn is somewhat larger than $\langle r_x^2 \rangle$. Lowering the temperature to 25 °C causes all values to increase, but $\langle r_x^2 \rangle$ increases so much that its values are now significantly larger than $\langle r_z^2 \rangle$.

For longer chains, the values of $\langle r_x^2 \rangle$, $\langle r_y^2 \rangle$, and $\langle r_z^2 \rangle$ are very similar, indicating that the end-to-end vector is nearly symmetrically disposed about each axis. At 25 °C, all these values have increased, with $\langle r_x^2 \rangle$ increasing more than $\langle r_y^2 \rangle$ and $\langle r_z^2 \rangle$. The picture for the fourth moments is qualitatively similar and again suggests a rather symmetrical distribution of $\mathbf{r}$ about the axes. These values reinforce the idea that the chains become somewhat more extended at lower temperature.

The Distribution of the End-to End Vector. A more illustrative description of the spatial arrangement of chains appears in plots of the density of chain ends along each of the three principal axes, $W(\mathbf{r}_i)$ ($i = x, y, z$). These supplement the average moments of the end-to-end vector $\mathbf{r}$ in detailing effects such as excluded volume or temperature on chain conformations.

As a consequence of the threefold rotational potential about each carbon–carbon bond in a polymethylene chain the distribution of the end-to-end vector is not a continuous function of distance, except in the limit of very long chains. Models which sample descrete chains accentuate this property of short polymers. Even very sophisticated models, like that of Lal and Spencer,[7] which allow energy-weighted rotational states different from gauche and trans, give distributions of $\mathbf{r}$ for relatively short chains which are not continuous.[8] As an aid to visualization, the points which represent the distribution of $\mathbf{r}$ or its projection on the principal axes are connected with lines.

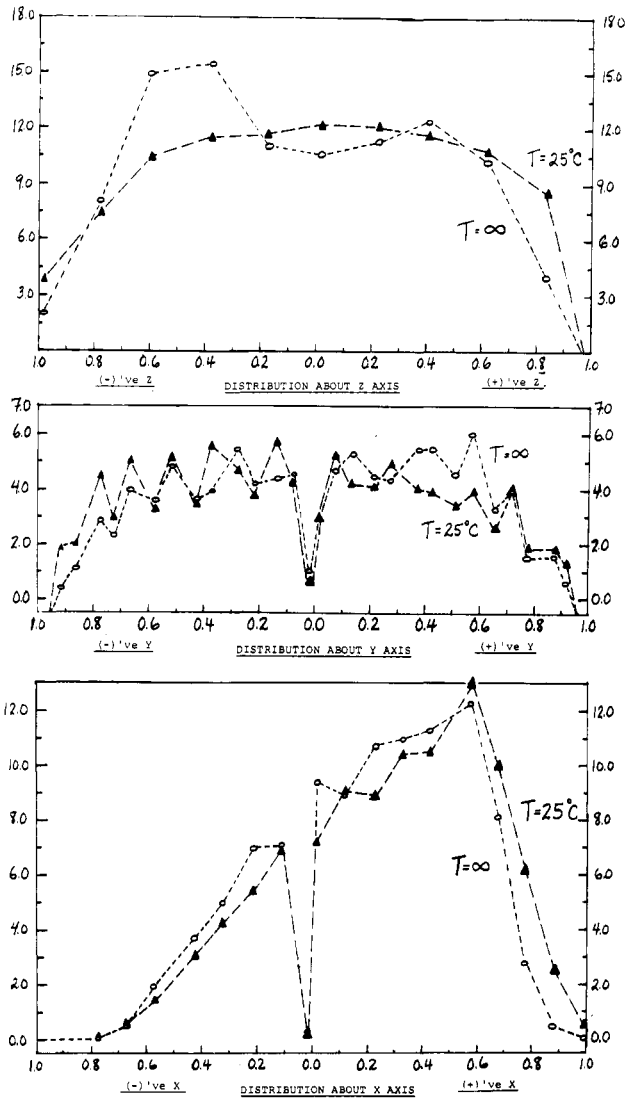

Figure 3. Distribution of the projections of the end-to-end vector on the axes of the right-handed Cartesian coordinate system shown in Figure 1. Values on the abscissia are given as $(\mathbf{r}_i/\mathbf{r}_{i,\max})$, $i = x, y, z$; ordinate values are in percent. Results are shown for 10-carbon chains at 25 °C and $T = \infty$ ($E_t = E_g$).

Figures 3, 4, and 5 show plots of $W(\mathbf{r}_i)$ against $(\mathbf{r}_i/\mathbf{r}_{i,\max})$ for 10-, 20-, and 30-carbon chains, respectively. The open circles refer to the condition $E_g = E_t$ and describe random walks on the lattice with second neighbor exclusions. The closed triangles refer to real chains at 25 °C. In each case the distribution along the x axis, $W(\mathbf{r}_x)$, favors positive values of $(\mathbf{r}_x/\mathbf{r}_{x,\max})$. The effect is more pronounced for 10-carbon chains, as a result of the ester group excluding volume from the first few methylene groups in the chain. As chain length increases to 20 and 30 carbons, the effect diminishes so that the plots of $W(\mathbf{r}_x)$ become more symmetrical. Even for 30-carbon chains, however, the graph has a maximum not at the origin but at a small positive value of $(\mathbf{r}_x/\mathbf{r}_{x,\max})$.

The distributions about the y and z axes, for unreweighted chains, have much less asymmetry. Short chains show slightly higher chain end density in the positive y and negative z di-

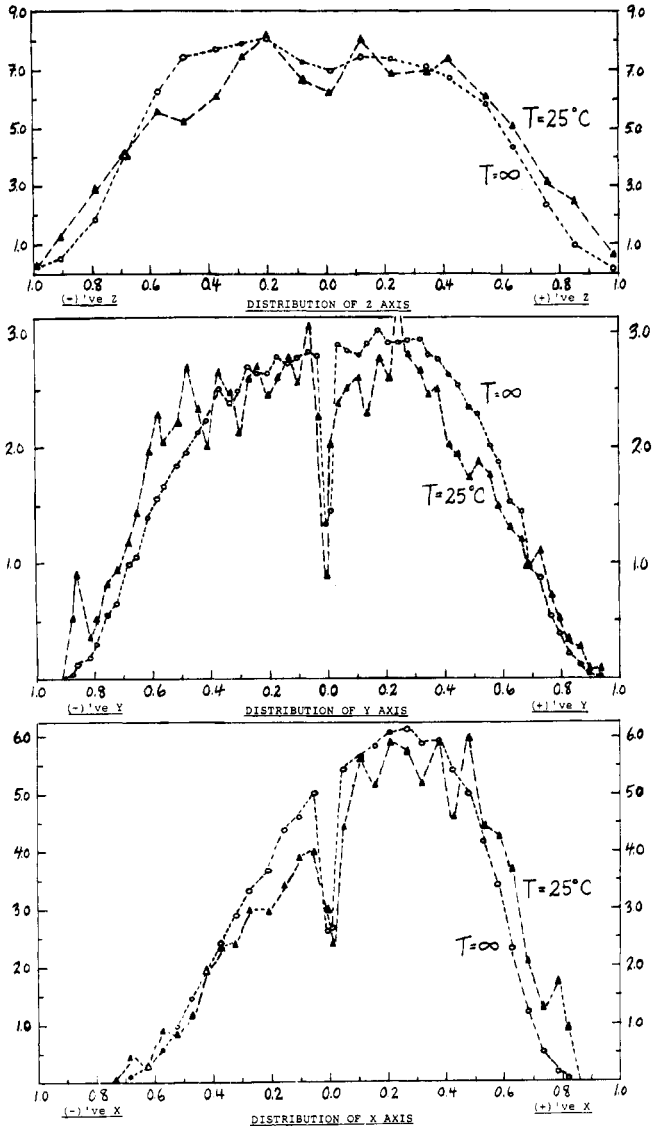

Figure 4. Distribution of the projections of **r** onto the principal axes for 20-carbon chains.

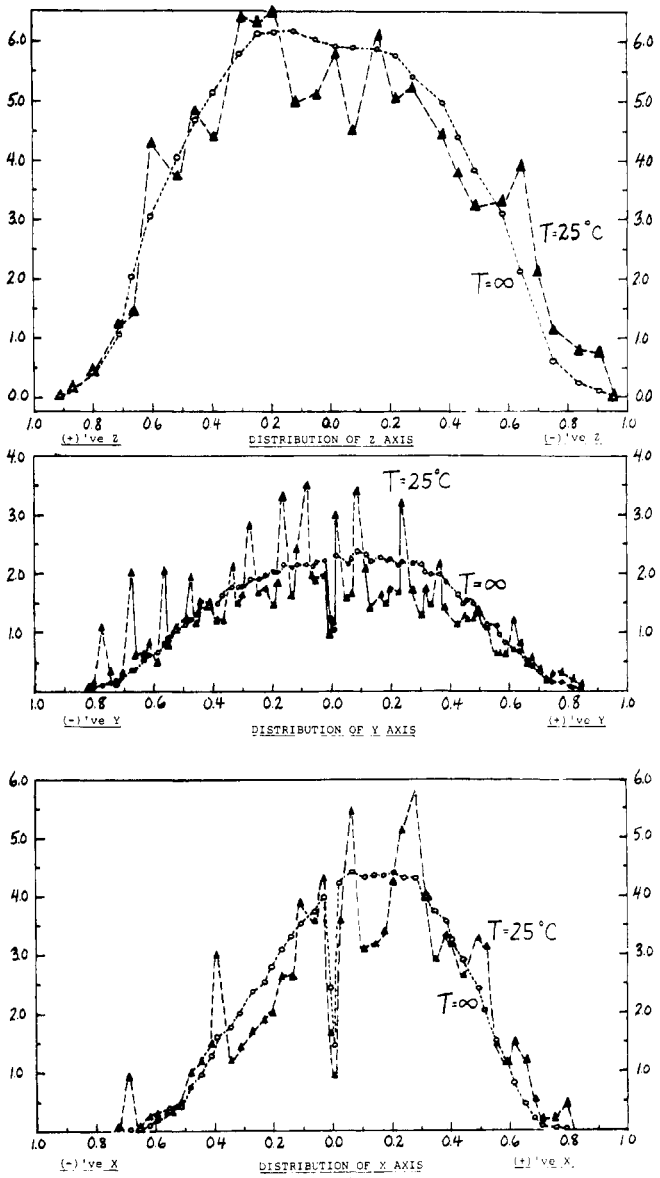

Figure 5. Distribution of the projections of **r** onto the principal axes for 30-carbon chains.

rections. Reweighting the chains to 25 °C results in an increased density of chain ends far from the origin and a jaggedness in $W(\mathbf{r})$, most pronounced for 30-carbon chains. The jaggedness at 25 °C is an interesting effect but it is hard to know whether it is real. The errors associated with the reweighted distribution range from 15 to 40% of the estimate and are particularly large for 30-carbon chains.

The most notable characteristic of the plots is the presence of a sharply defined minimum in $W(\mathbf{r})$ about the x and y axes, which is not found in the distribution about the z axis. It is most notable for 10- and 20-carbon chains, although an indication of its presence remains even for 30-carbon chains.

Fixman and Alben[9] have reported a similar effect in their attempts to describe analytically the shape of $W(\mathbf{r})$ for chains of less than 40 steps. They attributed this minimum to the stiffness of short chains. Others who have noted this effect for short chains are Flory and Yoon[2b] in their rotational isomeric studies of polymethylene chains and Domb et al.[2c] in lattice-based exact enumeration studies of self-avoiding walks on the simple quadratic and simple cubic lattices.

In the present case, attaching the benzophenone group to the chain excludes all ways of returning to the origin, so that $W(\mathbf{r})$ would be zero. Our studies, however, differ from Fixman's in that the distribution along each axis was studied separately. The finite value of the minimum results from chains attaining a zero value along one coordinate axis, while having large values for the other two coordinates.

It is tempting to explain the minima as an effect caused by the presence of the substituent. The effect is not observed for $\mathbf{r}_z$, and the substituent has virtually no thickness perpendicular to the x,y plane. A full understanding of the effect will come only from comparison with unsubstituted chains examined within the context of the same model and coordinate system.

The Fraction of Trans Bonds in Terminally Substituted Chains. Smith[10a,b] has exactly enumerated the conformations of chains up to 18 carbons grown on the diamond lattice, excluding all configurations with overlapping carbons or hydrogens. He compared the chain length dependence of the average fraction of trans bonds $\langle f_t \rangle$ and average mean-squared end-to-end distance $\langle r^2 \rangle$, with results from chains which exclude only GG′ configurations of five-carbon atoms. Exclusion of configurations with higher order interactions had no effect on these two properties of the chains. Moreover, the limiting value of $\langle f_t \rangle$ (determined by extrapolation to infinitely long chains) was quite similar to that calculated ana-

Table IV
Average Number of Gauche Bonds in Hydrocarbon Chains Attached to the Benzophenone 4-Carboxylate Substituent

Chain length	Av no. of gauche bonds	Stand[a] dev
1	0.00	
2	0.67	
3	1.25	
4	1.87	
5	2.32	
6	2.82	0.01
7	3.30	0.01
8	3.89	0.01
9	4.30	0.02
10	4.80	0.02
11	5.29	0.03
12	5.79	0.03
13	6.28	0.03
14	6.78	0.04
15	7.27	0.04
16	7.77	0.05
17	8.26	0.05
18	8.76	0.06
19	9.25	0.06
20	9.76	0.07
21	10.26	0.07
22	10.75	0.08
23	11.25	0.08
24	11.75	0.09
25	12.25	0.10
26	12.74	0.10
27	13.24	0.11
28	13.73	0.11
29	14.23	0.12
30	14.72	0.13

[a] Blank spaces imply $\sigma < 0.01$.

lytically by Nagai and Ishikawa,[11] assuming only GG′ interactions are excluded.

We wished to examine the effect of the terminal substituent on the fraction of gauche and trans rotamers in the chain. Table IV contains estimates of the number of gauche bonds in chains of 7 to 30 carbons attached to the benzophenone carboxylate substituent. Because of the presence of the ester group, the O–C_1 and C_1–C_2 bonds may be designated gauche or trans, and calculations of chain properties must take the energies of these orientations into account. For the purpose of comparing our data with Smith's calculation's on unsubstituted alkane chains, we need to correct our data appropriately. From the average number of gauche bonds in an n-carbon chain, it is necessary to subtract the contribution due to the first two bonds and normalize by the remaining number of bonds $(n - 2)$ in the chain. This gives the average fraction of gauche bonds $\langle f_g \rangle$, from which the fraction of trans bonds is obtained from $\langle f_g \rangle + \langle f_t \rangle = 1$. These results are plotted in Figure 6, along with Smith's data for unsubstituted chains, as a function of the inverse of the chain length, n^{-1}.

Terminally substituted chains show higher $\langle f_t \rangle$ values for shorter chains, although the increase is only about 2% of the $\langle f_t \rangle$ value for unsubstituted chains. This may reflect exclusion of configurations interacting with the ester group and the chromophore. Both plots extrapolate to the same limiting

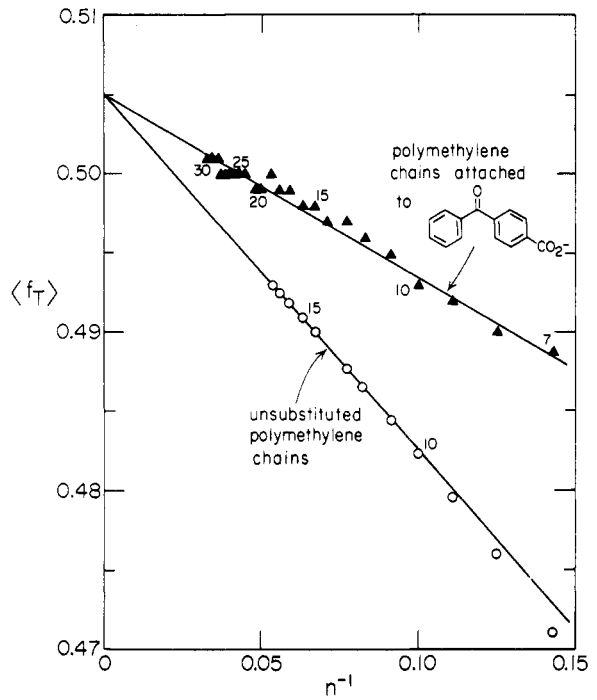

Figure 6. Comparison of the fraction of trans bonds as a function of chain length for (Δ) chains attached to benzophenone 4-carboxylate and for (○) unsubstituted chains. Both sets of data refer to walks on a diamond lattice with second-neighbor exclusions. The data for unsubstituted chains come from exact enumeration studies by Smith, ref 3.

value of 0.505, very close to the 0.5 value calculated by Nagai and Ishikawa (with a different model) for infinitely long chains. It appears that volume excluded by the benzophenone group has only a small affect on the fraction of trans totamers in the chain.

Acknowledgment. The authors wish to thank the Research Corporation and the National Research Council of Canada for their generous financial support.

References and Notes

(1) P. J. Flory, "Statistical Mechanics of Chain Molecules", Interscience, New York, N.Y., 1969.
(2) (a) F. T. Wall and R. A. White, *Macromolecules*, **7**, 849 (1974); (b) D. Y. Yoon and P. J. Flory, *J. Chem. Phys.*, **61**, 5366 (1974); (c) C. Domb, J. Gillis, and G. Wilmers, *Proc. Phys. Soc., London*, **85**, 625 (1965).
(3) (a) K. Zachariasse and W. Kühnle, *Z. Phys. Chem. (Frankfurt am Main)*, **101**, 267 (1976); (b) N. Boens, M. DeBrackeleire, J. Huybrechts, and F. C. DeSchryver, *ibid.*, **101**, 417 (1976); (c) C. Galli, G. Illuminati, L. Mandolini, and P. Tamborra, *J. Am. Chem. Soc.*, **99**, 2591 (1977); (d) K. Shimada and M. Szwarc, *ibid.*, **97**, 3313, 3321 (1975); (e) Y. Sato, H. Nakai, T. Mizoguchi, Y. Hatanaka, and Y. Kanaoka, *ibid.*, **98**, 2349 (1976).
(4) D. S. Saunders and M. A. Winnik, *Macromolecules*, following paper in this issue.
(5) M. A. Winnik, *Acc. Chem. Res.*, **10**, 178 (1977).
(6) (a) M. N. Rosenbluth and A. W. Rosenbluth, *J. Chem. Phys.*, **23**, 356 (1955); (b) F. L. McCrackin, J. Mazur, and C. M. Guttman, *Macromolecules*, **6**, 859 (1973).
(7) M. Lal and D. Spencer, *Mol. Phys.*, **22**, 649 (1971).
(8) R. J. J. DeKanter, R. Kaptein, and R. A. Van Sauter, *Chem. Phys. Lett.*, **45**, 575–9 (1977).
(9) M. Fixman and R. Alben, *J. Chem. Phys.*, **58**, 1553 (1973).
(10) (a) R. P. Smith, *J. Chem. Phys.*, **40**, 2963 (1964); (b) **42**, 1162 (1965); (c) **47**, 5364 (1964).
(11) K. Nagai and T. Ishikawa, *J. Chem. Phys.*, **37**, 496 (1962).
(12) Taken from the M.Sc. Thesis of D.S.